

Numerical analysis on the effect of varying number of diffuser vanes on impeller - diffuser flow interaction in a centrifugal fan *

K. Vasudeva Karanth , N. Yagnesh Sharma[†]

Department of Mechanical & Mfg. Engineering, Manipal University, Manipal, India

Abstract. It is quite well known that the diffusers are required for efficient conversion of the dynamic head generated by the impeller in a centrifugal fan. Hence the flow into the diffuser passage plays a crucial role in determining the efficiency of conversion. The flow in the region bounded by the impeller exit and the diffuser entry i.e. the radial clearance space is generally considered to be highly complex. With the development of PIV as well as versatile numerical CFD tools such as moving mesh techniques, it has become possible to arrive at a prudent solution compatible with the physical nature of the flow. Hence, in this work a numerical solution with moving mesh technique is made use of in predicting the real flow behavior, as exhibited when a target blade of the impeller is made to move past a target blade on the diffuser. Many research works both experimental and numerical on the impeller diffuser interactive phenomenon have been undertaken so far. But it is found from the literature that the study on the impeller diffuser interaction as well on the performance of the fan by varying the number of diffuser vanes has not been the focus of attention in these works. Hence a numerical analysis has been carried out in this work to extensively explore impeller-diffuser fluid interaction as well as to predict the flow characteristics of the fan by changing the number of diffuser vanes while keeping the number of impeller blades same. It is found from the analysis that there is an optimum number of diffuser vanes which would yield maximum static pressure recovery and when the diffuser vanes are increased beyond certain number, rotating stall occurs in diffuser flow passages corresponding to the blade passing frequency. Further it is observed from the analysis that smaller the number of diffuser vanes, larger is the pressure fluctuations at the exit flange of the fan which eventually would even out as the number of diffuser vanes are increased.

Keywords: sliding mesh, unsteady flow, impeller-diffuser interaction, rotating stall, optimum number of diffuser vanes

1 Introduction

With the rapid development of online flow measuring systems like PIV and parallel development in CFD, a large number of research efforts are underway to explore the intricacies of whole field flow within a Turbomachine. Hence a significant number of research articles^[2-14, 16] are available which explicitly explore the impeller diffuser interactive phenomenon by both experimental and numerical methods. Ubaldi et al.^[14] attributed principal cause of the high loss levels observed in the diffuser due to the strong span-wise distortion in swirl angle at inlet which initiates a strong hub/corner stall. Tsukamoto^[13] has calculated the unsteady flow caused by the interaction between impeller and diffuser vanes in a diffuser pump by using the singularity method. According to Justen et al.^[4] the time-dependent pressure distribution on the diffuser front wall and on the suction and pressure surfaces of the diffuser vanes reveal that the semi-vaned space mainly the region near

* The authors wish to acknowledge and thank Tarek Meakhail and Seung O Park, for readily giving the centrifugal fan drawing for our numerical modeling. They also wish to thank Manipal Institute of Technology, Manipal University, for providing computational resources for undertaking this study.

[†] Corresponding author. Tel.: +91-820-2571061; fax: +91-820-2571071. E-mail address: nysharma@hotmail.com.

the vane suction side is influenced by the unsteady impeller-diffuser interaction and that the pressure fluctuations appear to be distinctly higher than the pressure fluctuations in the vaneless space. Sinha et al.^[10, 11] have carried out quantitative visualization of centrifugal pump with diffuser vanes. Shi and Tsukamoto^[9] in their study have shown that the Navier-Stokes code with the k- model is found to be capable of predicting pressure fluctuations in the diffuser. In a study by Meakhail et al.^[6] an attempt has been made to help understand the complex unsteady flow associated with the interaction between the impeller and its vaned diffuser. Sano et al.^[8] have carried out numerical study of flow instabilities in a vaned diffuser due to rotating stall, alternate blade stall, and asymmetric stall. In their two-part paper, Ziegler et al.^[16] have presented an experimental investigation of the effect of impeller-diffuser interaction on the unsteady flow and the time-averaged flow field in the interactive region of impeller and diffuser. Akinori and Hisasada^[2] have investigated the pressure fluctuations in the downstream of the vaned diffuser of a centrifugal pump impeller where they found the potential interaction between the impeller and the diffuser blades more strongly than the impeller-wake interaction. Michael^[7] has carried out a comparative study of unsteady flow in a transonic centrifugal compressor with vane-less and vaned diffusers. A part of the current work is validated with the results obtained by Meakhail and Park^[5], in which they explore the study of impeller-diffuser-volute interaction in a centrifugal fan. They report measurement data in the region between the impeller and vaned diffuser and have obtained results of numerical flow simulation of the whole machine. Jianjun et al.^[3] have carried out numerical simulations on impeller-diffuser interactions in radial diffuser pumps to investigate the unsteady flow and pressure fluctuations on the blade and vane surfaces. Different operating points, blade number configurations, and radial gaps between the impeller and diffuser have been examined to study their effects on the unsteady flow. They have found that flow rate, blade number configuration, and radial gap influence significantly the pressure fluctuation and associated unsteady effects in the diffuser pumps. Sofiane et al.^[12] have carried out the numerical unsteady flow analysis in a vaned centrifugal fan. According to Yahya^[15] for a higher pressure ratio across the radial diffuser, the diffusion process has to be achieved across a relatively shorter radial distance. This requires the application of vanes which provide greater guidance to the flow in the diffusing passages.

It can be observed from the above literature survey that the effect of number of diffuser vanes on the system performance as well as on the Impeller-Diffuser interaction in a centrifugal fan has not been explored well so far. Hence a numerical modeling of the flow domain which includes a portion of the inlet to the impeller as well as the diffuser along with volute casing has been carried out and moving mesh technique has been adopted for unsteady flow simulation of the centrifugal fan in this work.

2 Numerical modelling

2.1 Geometry and grid generation

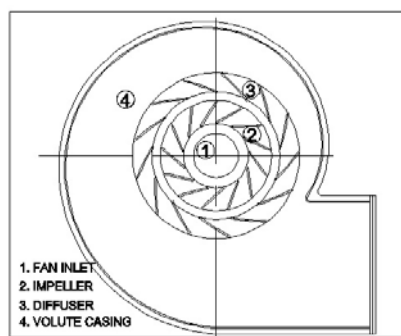
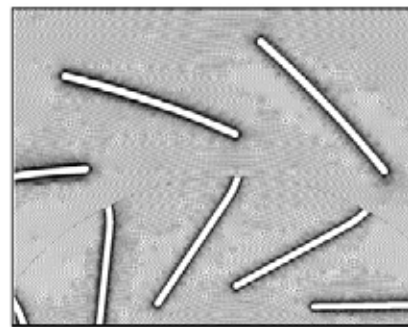
The centrifugal fan stage consists of an inlet region, an impeller, a vaned diffuser, and a volute casing (Fig. 1). The impeller consists of thirteen 2-D backward swept blades with an exit angle of 76° relative to the tangential direction. The radial gap between the impeller outlet and diffuser inlet is 15% of the impeller outlet radius. All the blades are of 5 mm thickness. The specifications of the fan stage are shown in Tab. 1.

The technical paper by Meakhail and Park^[5] forms the basis for geometrical modeling in the present work. The model of the fan consists of four parts, the inlet, the impeller, the diffuser and the volute region. Unstructured meshing technique is adopted for establishing sliding mesh configuration as the analysis is unsteady as per CFD code^[1]. The grid for the volute part of the domain has 163,590 nodes and 162,113 quad elements. The diffuser has 163,213 nodes and 155,106 quad elements. The impeller has 80,971 nodes and 74,143 quad elements. The inlet part of the domain has 5,536 nodes and 5,190 quad elements respectively. The maximum size of the element is limited to elements having an edge length of 2 mm. However to establish grid independency a finer model having an element edge length of maximum of 1 mm is carried out and the variation in the results were found to be less than 1.5% and hence to save the computational time, elements edge length of maximum 2 mm size is adopted.

Fig. 2 shows the meshed domain and it can be observed that a finer mesh is adopted near the surface of the impeller and diffuser vanes to capture the boundary layer effects using a suitable sizing algorithm as provided in CFD code^[1].

Table 1. Please write your table caption here

Impeller inside radius r_1	120 mm
Impeller outside radius r_2	200 mm
Diffuser inside radius r_3	230 mm
Diffuser outside radius r_4	300 mm
Exit flange width	450 mm
Width of diffuser blade	35 mm
Width of volute casin	90 mm
Impeller inlet vane angle	30°
Impeller outlet vane angle	76°
Diffuser inlet vane angle	23°
Diffuser outlet vane angle	38°
Number of impeller vanes	13
Number diffuser vanes	13
Speed of the fan	1000 rpm

**Fig. 1.** Model of the centrifugal fan**Fig. 2.** Meshed domain of the fan

2.2 Unsteady calculations setup

Two-dimensional, unsteady Reynolds-averaged Navier- Stokes equations set to polar coordinate system are solved by the CFD code^[1]. To obtain the flow characteristic and efficiency curves of the fan, total pressure (gage) is applied at the inlet and static pressure (gage) is applied at the flange exit as the boundary conditions. However for comparing the configurations with different radial clearances, an absolute velocity of 5 m/s which corresponds to the design point mass flow rate is imposed at the inlet and a zero gradient outflow condition of all flow properties is applied at the flange exit of the fan, assuming fully developed flow conditions.

A no-slip wall condition is specified for the flow at the wall boundaries of the blades, the vanes, and also the volute casing. The turbulence is simulated using a standard $k - \epsilon$ model^[1]. Turbulence intensity of 5% and a turbulent length scale of 0.5 m which is the cube root of the domain volume are adopted in the study. The unsteady formulation used is a second order implicit velocity formulation and the solver is pressure based^[1]. The pressure-velocity coupling is done using SIMPLE algorithm and discretization is carried out using the power law scheme. The interface between the impeller and the diffuser is set to sliding mesh in which the relative position between the rotor and the stator is updated with each time step. The time step Δt is set to 0.0001 s, corresponding to the advance of the impeller by $\Delta\gamma = 0.610$ rad per time step for a rated speed of 1000 RPM to establish stability criterion. The maximum number of iterations for each time step is set to 30 in order to reduce all maximum residuals to a value below 10^{-5} . Since the nature of flow is unsteady, it is required to carry out the numerical analysis until the transient fluctuations of the flow field become time periodic as judged by the pressure fluctuations at salient locations in the domain of the flow. In the present analysis this has been achieved after two complete rotations of the impeller. The salient locations chosen are the surfaces corresponding to the inlet duct to the impeller, impeller exit, diffuser exit, on impeller vanes and on diffuser vanes and the exit flange of the volute casing. The time and area weighted averages for the pressure and velocity fluctuations at each salient location in the computational domain are recorded corresponding to each rotation of the impeller by time step advancement. To analyze the flow characteristics through the impeller

and diffuser vanes as well as the performance of the fan, two coefficients are used: the static pressure recovery coefficient and the total pressure loss coefficient. These are calculated based on the weighted averages^[1] and are plotted with respect to time steps for the diffusing domains of the fan.

$$\begin{aligned}\phi &= \text{Flow coefficient} = \left(\frac{Q}{\pi r_2^2 U_2} \right) \\ \psi &= \text{Head coefficient} = \left(\frac{p_4 - p_1}{\rho U_2^2} \right) \\ C_{opr} &= \text{Overall static pressure recovery coefficient} = \left(\frac{p_4 - p_2}{p_{t2} - p_2} \right) \\ K_{opr} &= \text{Overall total pressure loss coefficient} = \left(\frac{p_{t2} - p_{t4}}{p_{t2} - p_2} \right) \\ C_{dpr} &= \text{Diffuser static pressure recovery coefficient} = \left(\frac{p_3 - p_2}{p_{t2} - p_2} \right) \\ K_{dpr} &= \text{Diffuser total pressure loss coefficient} = \left(\frac{p_{t2} - p_{t3}}{p_{t2} - p_2} \right) \\ C_{fes} &= \text{Flange exit static pressure coefficient} = \left(\frac{p_4}{\rho U_2^2} \right)\end{aligned}$$

The numerical model for the whole field flow calculations is validated by calibrating the results of the current

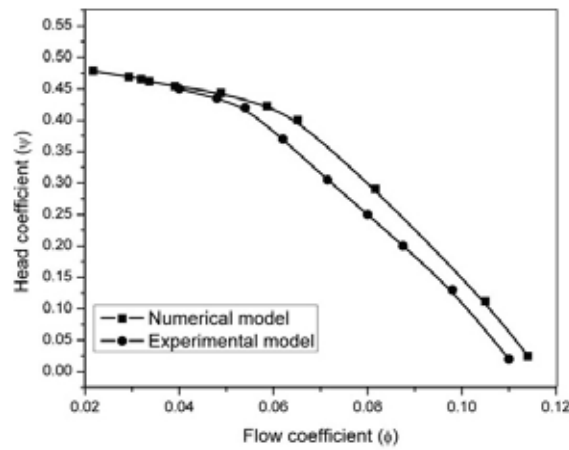


Fig. 3. Validation characteristics curve for Head coefficient vs. Flow coefficient

numerical work with the experimental work carried out by Meakhail and Park^[5]. Fig. 3 shows the validation characteristics curve of Head coefficient with Flow coefficient. The characteristic graph captures the validation results for the current work with the work cited above. The plot shows a decrease in the head coefficient as the flow coefficient increases as is required for a backward swept impeller blade. The validation shows a close agreement between the present numerical model and the experimental model of Meakhail and Park^[5].

2.3 Geometric configurations for the number of diffusers.

The basic configuration for varying the number of diffuser vanes is the configuration having 13 blades on both the impeller and diffuser and with a radial gap of 30 mm between them. The diffuser vanes are varied from 5 to 14 vanes, while the number of impeller blades is kept constant at 13.

3 Results and discussion

The flow leaving the impeller has jets and wakes. When such a flow enters a large number of diffuser passages, the quality of flow entering the diffuser vanes differs widely and some of the vanes may experience flow separation leading to rotating stall and poor performance. To avoid such a possibility, it is suggested to provide a smaller number of diffuser vanes than that on the impeller^[15]. When the number of vanes is reduced, the angle of diffusion for each vane passage becomes larger. Now, at larger diffusing angle of the passage the

static pressure conversion is more but attended by fluid flow losses due to poorer flow guidance. When the number of vanes is increased the angle of diffusion decreases and hence the static pressure conversion reduces but the flow losses tend to decrease due to better guidance but is offset partially by skin friction losses due to the larger contact surfaces of increased number of diffuser vanes. Hence there is a need to arrive at a trade off with respect to the number of diffuser vanes vis--vis the fluid guidance and friction effects in the blade passages.

Fig. 4 shows the static pressure contour plots for diffuser configurations with odd number of vanes. It is clearly seen from the contour plots that for diffuser with lower number of vanes (5 vanes), static pressure at the diffuser exit is quite large compared to diffuser with larger number of vanes (11 vanes). The reason for this could be attributed to fairly large angle of diffusion provided for diffuser with lower number of vanes as stated earlier. Since the number of diffuser vanes are less, the flow passage is wider and hence, the presence of recirculating flow disturbances do not affect the through flow in the diffuser vane passage, but diffusion process will be affected due to lower flow guidance within passage as explained earlier. Similarly Fig 5 shows static pressure contour plots for diffuser with even number of vanes. A similar trend as explained above occurs with static pressure distribution being higher for smaller number of vanes. However a careful study of the odd and even number combinations of diffuser vanes reveals that the odd number of diffuser vanes provides a better recovery of static pressure than the even number of vanes. A possible reason for the above observed fact may be that since the impeller is made of odd number of blades which is unchanged in the analysis, the diffuser with even number of blades has flow mismatch leading to greater incidence losses. Fig. 6 and Fig. 7

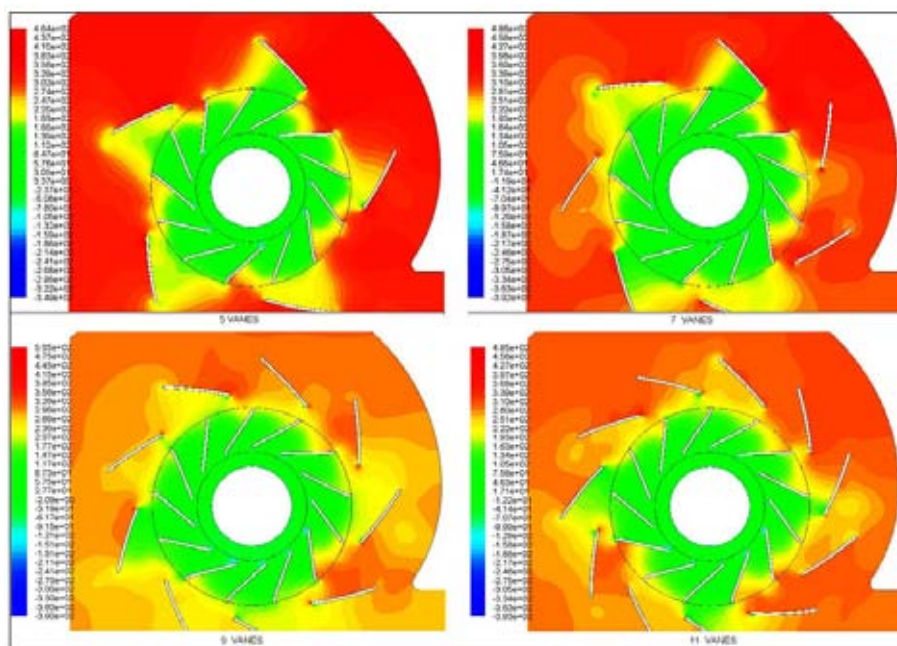


Fig. 4. Static pressure contour plots for configuration with odd number of diffuser vanes.

show instantaneous vector plots of velocity, colored according to its magnitude. The recirculation zones on the impeller and diffuser suction sides are clearly visible for all the configurations. The influence of rotating stall comes into force for diffuser vanes with larger number of vanes (10 to 14 vanes). The reasons for this are two fold: Firstly the stalling phenomenon is associated with the blade passing frequency. With larger number of vanes on the diffuser, the blade passing frequency increases leading to rotating stall. Secondly this occurrence is due to narrower vane passages of the diffuser in which recirculation on the suction side of the diffuser vanes gets converted into a rotating stall. This phenomenon is well recorded in literature^[8] at the exit flange of the fan.

Fig. 8 and Fig. 9 show the static pressure recovery coefficient for odd and even number diffuser vanes. It can be observed from these figures that the diffuser static pressure recovery coefficient increases with in-

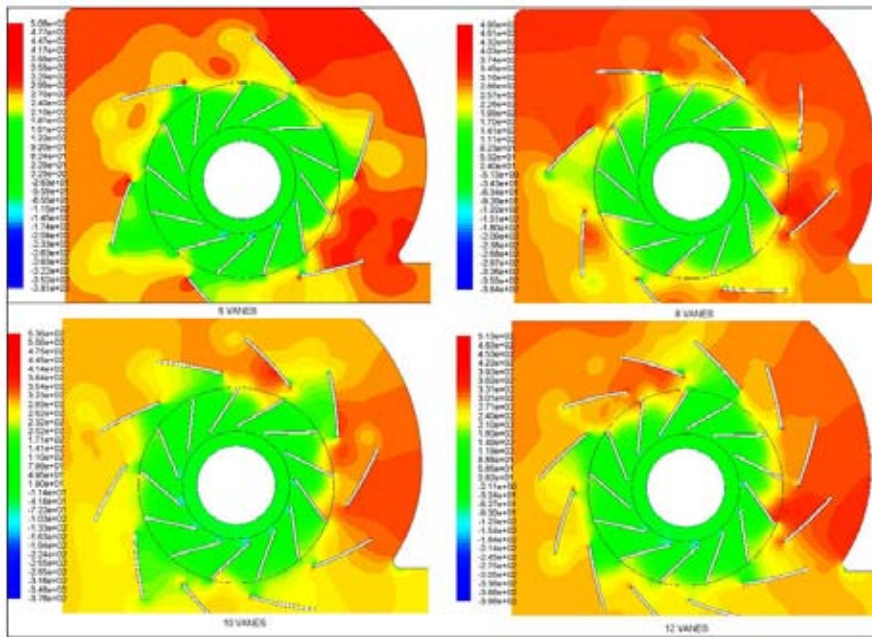


Fig. 5. Static pressure contour plots for configuration with even number of diffuser vanes.

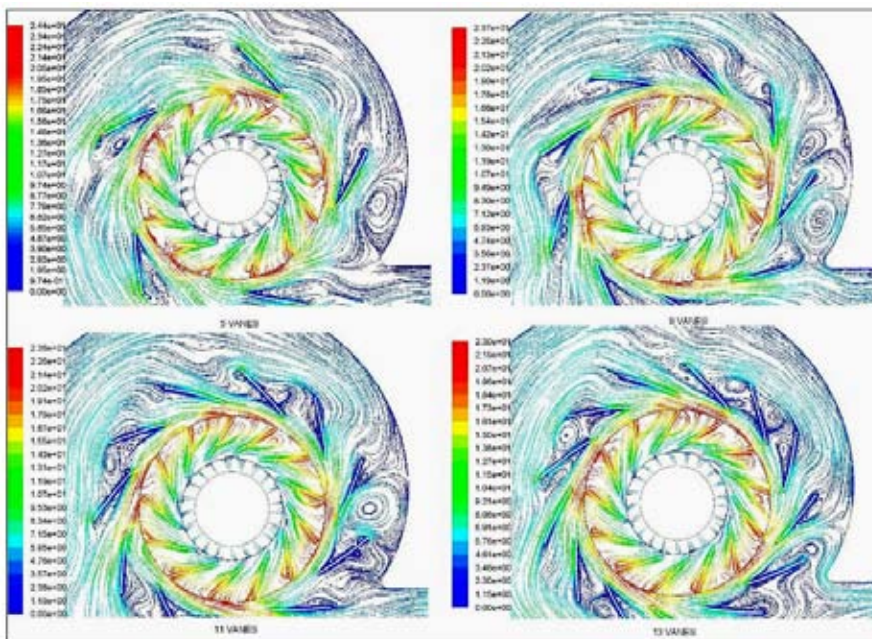


Fig. 6. Instantaneous velocity vector plots for configuration with odd number diffuser vanes.

crease in vanes upto 9 or 10 vanes depending on whether it is odd or even configuration respectively. These coefficients then tend to decrease with increase in number of vanes. The reason for this can be explained as follows. With lower number of vanes the diffusion process is affected by poorer flow guidance of the fluid particles even though the diffusion angle is large. As the flow guidance improves with increase in number of vanes, the surface friction will also correspondingly increase. Fig. 10 and Fig. 11 show the total pressure loss coefficient for odd and even number vanes respectively. Hence beyond 9 or 10 vanes the flow losses due to surface friction overtakes the static pressure recovery, though there is better guidance of fluid. From the above considerations it seems as far as the number of diffuser vanes is concerned, there is a trade-off between the number of diffuser vanes and the total pressure loss coefficient.

Fig. 8 and Fig. 9 also show the overall static pressure recovery coefficient for odd and even number of diffuser vanes. The overall static pressure recovery coefficient, which measures the static pressure recovery

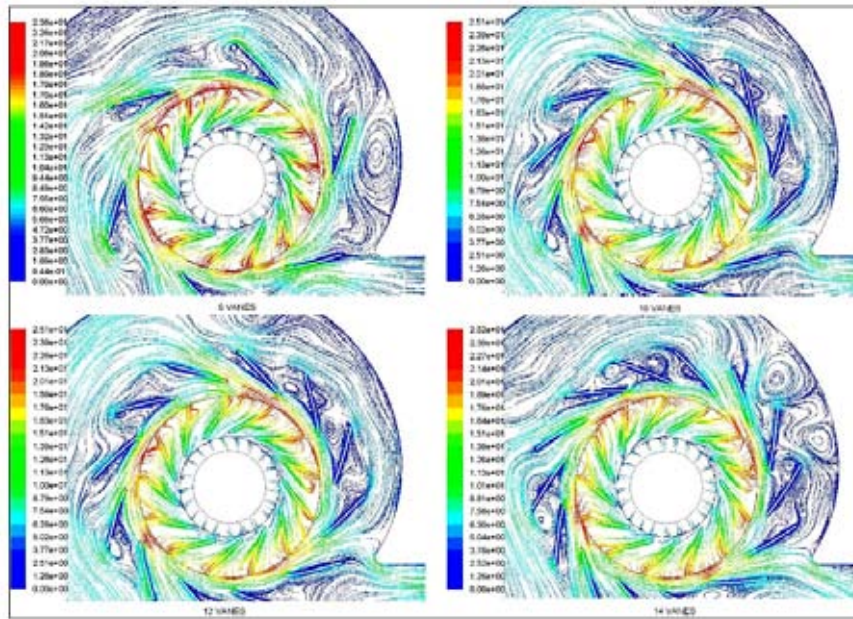


Fig. 7. Instantaneous velocity vector plots for configuration with even number of diffuser vanes.

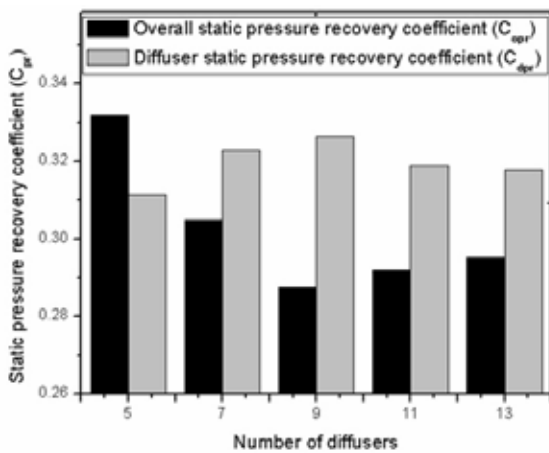


Fig. 8. Instantaneous velocity vector plots for configuration with even number of diffuser vanes.

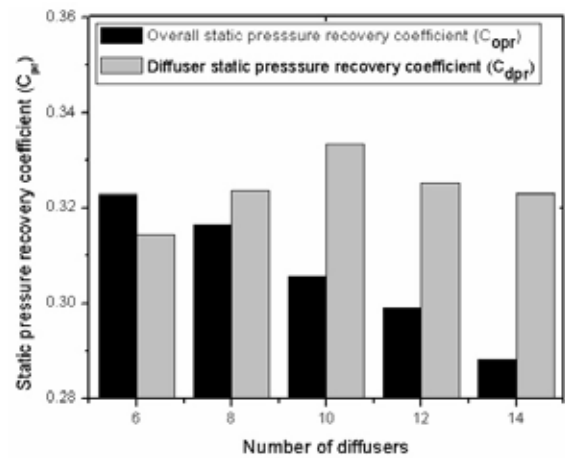


Fig. 9. Instantaneous velocity vector plots for configuration with even number of diffuser vanes.

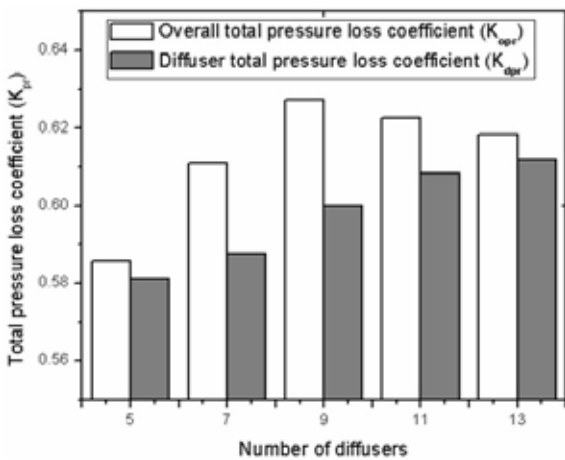


Fig. 10. Total pressure loss coefficient for odd number diffuser vanes.

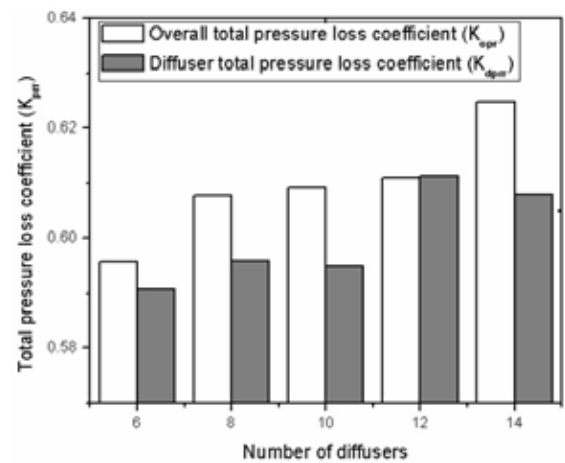


Fig. 11. Instantaneous velocity vector plots for configuration with even number of diffuser vanes.

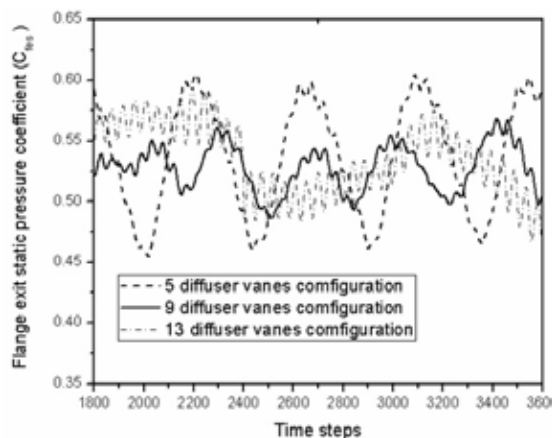


Fig. 12. Total pressure loss coefficient for odd number diffuser vanes.

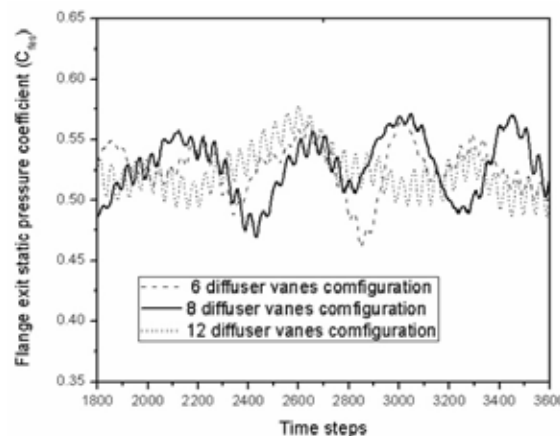


Fig. 13. Instantaneous velocity vector plots for configuration with even number of diffuser vanes.

from the impeller exit to the volute flange exit, decreases with increase in number of diffuser vanes. This is due to the fact that with the increase in number of diffuser vanes, the diffusing space becomes narrower and angle of diffusion also decreases leading to the formation of recirculation zones. This flow disturbance causes non uniform flow to enter the volute region. Due to these non uniform flows entering the volute region from the diffuser there is a greater total pressure loss in the volute region. From these figures it is also observed that larger overall static pressure recovery coefficient occurs for the diffuser with lower number of vanes and also that the odd number of diffuser vanes have better conversion compared to diffusers with even number of vanes. Fig. 12 and Fig. 13 show the static pressure fluctuations at the exit flange of the fan with time and it can be observed that the fluctuations die down with increase in number of diffuser vanes. This is due to the fact that the increased number of diffuser vanes cause better flow guidance leading to reduced pressure fluctuations

4 Conclusion

The following conclusions are derived from the analysis carried out in this paper:

- (1) There is an optimum number of diffuser vanes which would develop maximum static pressure recovery. This corresponds to 9 vanes for diffuser with odd number of vanes and 10 vanes corresponding to even number of vanes in the present analysis.
- (2) The rotating stall occurs in some of the alternate flow passages of the diffuser and this problem exists only when the number of diffuser vanes increase beyond a certain number (which happens to correspond to 10 vanes in the present work)
- (3) The odd number of diffuser vanes provide a better recovery of static pressure than the even number of vanes.
- (4) It is also contra indicating that static pressure reduction occurs in the volute casing when number of diffuser vanes are increased.
- (5) The overall static pressure recovery coefficient, which also takes into account the volute region of the fan, decreases with increase in number of diffuser vanes.
- (6) The amplitude of static pressure fluctuations at the exit flange decreases with increase in number of diffuser vanes

5 Nomenclature

p	Static pressure (Pa)
p_t	Total pressure (Pa)
U_2	Tangential velocity at impeller exit (m/s)
ρ	Air density (kg/m^3)
Q	Volume flow rate (m^3/sec)
γ	The angle of advance of a given impeller blade to next successive blade position.
<i>suffix</i>	1-impeller inlet, 2-Impeller exit, 3-Diffuser exit, 4-Flange exit of the fan.

References

- [1] 2006. Fluent 6.3, Fluent Inc.
- [2] F. A. F, T. Hisasada. Pressure Fluctuation in a Vaned Diffuser Downstream from a Centrifugal Pump Impeller. *International Journal of Rotating Machinery*, 2003, **9**: 285–292.
- [3] J. Feng, F. Benra, H. Dohmen. Numerical investigation on pressure fluctuations for different configurations of vaned diffuser pumps. *International Journal of Rotating Machinery*, 2007, **2007**: 10.
- [4] F. Justen, K. Ziegler, H. E. Gallus. Experimental investigation of unsteady flow phenomena in a centrifugal compressor vaned diffuser of variable geometry. *ASME Journal of Turbomach*, 1999, **121**.
- [5] T. Meakhail, S. Park. A Study of Impeller-Diffuser-Volute Interaction in a Centrifugal Fan. *ASME J. Turbomach*, 2005, **127**: 84 – 90.
- [6] T. Meakhail, Z.Li, et al. The application of piv in the study of impeller diffuser interaction in centrifugal fan. part ii-impeller-vaned diffuser interaction. **in: Proceedings of The ASME Fluid Engineering Division- IMECE2001/FED-24953**, USA, 2001, 11–16.
- [7] M. Michael. Comparative Study of Unsteady Flows in a Transonic Centrifugal Compressor with Vaneless and Vaned Diffusers. *International Journal of Rotating Machinery*, 2005, **1**: 90–103.
- [8] T. Sano, Y. Yoshida, et al. Numerical Study of Rotating Stall in a Pump Vaned Diffuser. *ASME Journal of Fluids Engineering*, 2002, **124**: 363 – 370.
- [9] F. Shi, H. Tsukamoto. Numerical Study of Pressure Fluctuations caused by Impeller-Diffuser Interaction in a Diffuser Pump Stage. *Transactions of the ASME*, 2001, **123**: 466 – 474.
- [10] M. Sinha, J. Katz. Quantitative visualization of the flow in a centrifugal pump with diffuser vanes-i: on flow structures and turbulence. *Journal of Fluids Engineering*, 2000, **122**(1): 97–107.
- [11] M. Sinha, J. Katz, C. Meneveau. Quantitative visualization of the flow in a centrifugal pump with diffuser vanes-ii: addressing passage-averaged and large-eddy simulation modeling issues in turbomachinery flows. *Journal of Fluids Engineering*, 2000, **122**(1): 108–116.
- [12] K. Sofiane, K. Sma?ne. Flow study in the impeller-diffuser interface of a vaned centrifugal fan. *ASME J. Fluid Engineering*, 2007, **127**: 495 – 502.
- [13] H. Tsukamoto. Theoretical study of pressure fluctuations downstream of a diffuser pump impeller-part 1: Fundamental analysis on rotor-stator interaction. *ASME Journal of Fluids Engineering*, 1997, **119**: 647–652.
- [14] M. Ubaldi, P. Zunino, et al. An experimental investigation of stator induced unsteadiness on centrifugal impeller outflow. *ASME J of Turbomach*, 1996, **118**(1): 41–51.
- [15] S. Yahya. *Turbines Compressors and Fans*, 2nd edn. Tata McGraw Hill, 2005.
- [16] K. Ziegler, H. Gallus, R. Niehuis. A Study on Impeller-Diffuser Interaction-Part II: Detailed Flow Analysis. *ASME Journal of Turbomach*, 2003, **125**: 183 – 192.